Unsupervised Machine Learning Algorithm for Center Point Detection of Shear Reinforcement with Dual Anchorage

Hossain Mohammad Abul,
John Mlyahilu,
Hongseok Choi,
Jaeun Lee,
Youngbong Kim,
Jongnam Kim,
Division of Computer Engineering and AI
Pukyong National University, Busan, 48513, South Korea

***Abstract*—Welding activities are very hazardous to both clients and the environment such that they can cause damages during action whose impacts affect both the operators and evaluators. The situation happens when a breakdown occurs to the operating machines particularly self and manual-driven robots causing environmental pollution, injury, and sometimes death. Apart from that, products made through welding processes are instantly blazing such that they can cause skin burns and finger or toe cuts if no intelligent system is employed to assist the evaluators. In this study, we propose an unsupervised machine-learning algorithm for a mobile robot to grab, pick, and dispatch the shear reinforcement of dual anchorage (SRD) to the assembling part. The proposed algorithm uses a combination of image processing techniques and backward affine transformation to automatically detect the center point of an SRD. The image processing techniques are used for feature selection and extraction whereas the affine transformation is used to preserve the lines and parallelism but not necessarily the angles and distances. The experimental results show that the proposed algorithm worked better than the centroid, and the midpoint-based algorithms at an accuracy of 92% with an average speed of 0.025 seconds.**

Keywords—computer vision; affine transformation; parallel lines; gradients; convex hull

I. INTRODUCTION

The use of Shear Reinforcement of Dual-anchorage (SRD) in the field of building construction has been cited as a new paradigm shift that seems to be strong with huge potential as described by Do et al., in [1]. An SRD is defined as a cast-in-place reinforcement installed to increase the shear capacity of concrete which is not strong enough on its own [2]. The SRDs are used to increase and reach the strength of concrete by adding tension and compression force to the concrete made up through conventional methods such as cylindrical metal rods fused together with wire strips. Additionally, they strengthen the compression zone to allow the concrete to reach maximum strength by improving ductility. On the other hand, conventional methods such as cylindrical metal rods are said to be weak and their production is disadvantaged by time consumption. The SRDs are industrially made products through welding procedures whereby a complete SRD is made up by fusing together three (3) members with a filler material to form a structure. In this study, we introduce an SRD as a structure with four joints known as welding beads and the working environment through Fig. 1.

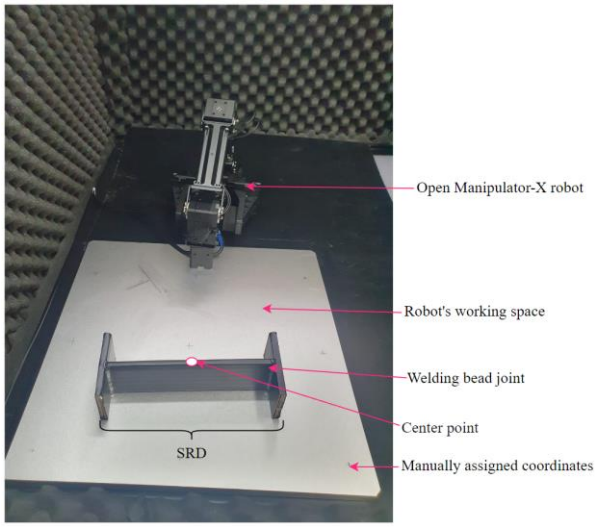

Fig. 1. SRD with four welding beads and midpoint.

From Fig. 1 above, four joints are made by connecting the three structures of an SRD. The evaluation of the welding bead joints is thoroughly described in [3-5] by using conventional algorithms such as active contours, thresholding, connected components, and Markov random fields, the algorithms are too many to list. Object detection algorithms are divided into two categories, the rule-based and the AI-based algorithms whereby within AI, the Machine learning-based algorithms are contained [6-7]. Rule-based algorithms for object detection normally perform better, however, they are prone to noise and usually mislead by exploding or vanishing gradient problems [8]. Unlike the rule-based ones, AI-based algorithms seem to be the best but they are easily misled to the wrong detection when the learning algorithm feels data deficient and sometimes subject to computational complexity causing them to be super slow in

real-time applications [9]. Therefore, in this study we propose a machine learning algorithm that detects the complete SRD and assigned the midpoint on it to be used by an open manipulator X arm robot for grabbing, picking, and dispatching it to an assembling part.

Lastly, we present the organization of this paper in sections including the introduction, related works, proposed algorithm, experimental results, and conclusion. This work is organized into five sections whereby Section II presents the related works and Section III presents the proposed algorithm with both mathematical background and its computational implementation diagrammatically. Section IV presents the experimental results and discussion whereas the conclusion reads last by describing the concluding remarks and limitations of the proposed algorithm.

II. Related Works

The studies on SRDs have been widely mentioned in mechanical and structural engineering for a decade up to date. As described in [2] and [8], SRDs exist in various models depending on the activities that they are meant for. The SRDs are nowadays used to build road bridges, mansions, statues, football pitches, harbors, arenas, and towers because of the strength they add to normal concretes [8] and [9]. The studies on SRD in building and construction are promising because their concretes are such stable that they can overcome natural calamities such as earthquakes and even non-atomic bomb explosions. Various methods that are used to inspect the quality of the welding beads which makes a complete SRD as stated in [3] and [10]. Additionally, [11], proposed a cross-section bead image prediction in laser keyhole welding of AISI 1020 steel using deep learning architectures and found that the performance was reasonably accurate by 93.6%.

Contour-based algorithms are used for segmentation because they detect and localize the object by providing a bounding box. The box contains information about where the object is located in a scene. The contour-based algorithms use energy force maximization subject to internal and external energy constraints [3-5]. They are widely used in many fields but they seem to be inferior to data with noise, easily trapped in local maxima in such a way that they are impractical for the detection of small objects. Apart from contour-based algorithms, there are supervised machine-learning algorithms for object detection. These algorithms include K-means clustering, and K-nearest neighborhood (K-NN). The advantages of K-Means are as follows; It is simple to implement and guarantees early convergence based on the desired number of clusters [6]. In the case of KNN, it is also simple to implement because it skips the training step [12]. It constantly evolves with new patterns in a dataset by learning non-linear decision boundaries. The two algorithms are outstanding however, they face some difficulties in data with high variance, causing their prediction for detection to be wrong.

Deep learning models are also useful in object detection because their accuracies rank at the top however, they require a lot of data to attain their superiority [13]. Additionally, pre-trained models like YOLO and mask RCNN provide a bounding that does not totally confine or enclose the object of interest rather, they give a level of confidence that an object is available or not [14]. With such limitations, this study avoids the use of contour-based and supervised machine learning algorithms because of the sensitivity of the data used. Based on the limitations of the datasets in this study, we could not employ supervised machine learning and deep learning algorithms to detect the SRD and extract the required information to be used for a robot. Therefore, we proposed an unsupervised machine learning algorithm for the detection of SRD, that calculates and assigns the midpoint of an SRD to be used by a mobile robot for grabbing, picking, and dispatching it to the assembling part.

III. Proposed Algorithm

The motivation for the proposed algorithm stems from the drawback experienced and exhibited by conventional algorithms like contour-based and connected components-based algorithms. First, the evolving contours normally do not realize the object borders in the image except if it gets close to it; therefore, they need curve or polygon initialization. Second, the contour cannot trail and survey the topological changes of the objects in an image freely without any parameter initialization. Therefore, to realize, address, and overcome the errors caused by the contour-based algorithms, we propose a machine learning algorithm that investigates the pixels of a gray and binarized image to obtain the center points to be used by a mobile robot for grabbing, and picking a welding bead through the center and dispatch it to the assembling part.

Let $G(x,y) \in \mathbb{R}^2$ be a gray image with dimension $W \times H$, where W is the width and H is the height of the image such that $I(x,y) \in [0,1]$ is a binary image indicating that 0 represents the black pixels and 1 represents the white pixels. Since $I(x,y)$ has non-homogeneous coordinates, we create homogeneous coordinate that maps $I(x,y)$ to $I(x,y,1)$ and present it as a system of linear equations in Eq. 1.

$$\begin{cases} a_{11}x + a_{12}y + z = \alpha \\ a_{21}x + a_{22}y + z = \beta \\ a_{31}x + a_{32}y + z = \gamma \end{cases} \tag{1}$$

We use an affine registration and solve a linear system based on the Gaussian reduction method to triangulate a matrix of a system of linear equations. To make the first column of the matrix with 1 element and the rest of the elements being 0, we subtract to each line a linear combination of the first row and second row and lastly, we apply the two previous steps iteratively to obtain a diagonal and upper triangulated matrix as shown through the set of linear systems in Eq. 2.

$$I(x,y,1) = \begin{bmatrix} 1 & \frac{a_{12}}{a_{11}} & \frac{1}{a_{11}} & | a \\ 0 & 1 & \frac{1-a_{21}\left(\frac{a_{12}}{a_{11}}\right)}{a_{22}-a_{21}\left(\frac{a_{12}}{a_{11}}\right)} & | b \\ 0 & 0 & 1 & | c \end{bmatrix}^{-1} (x', y', 1) \tag{2}$$

where $a = \frac{\alpha}{a_{11}}$, $b = \frac{\beta - a_{21}\left(\frac{a_{12}}{a_{11}}\right)}{a_{22}-a_{21}\left(\frac{a_{12}}{a_{11}}\right)}$ and $c = \frac{\gamma - a_{31}\left(\frac{\alpha}{a_{11}}\right) - \left(a_{32}-a_{31}\left(\frac{a_{12}}{a_{11}}\right)\right)\times\left(\frac{\beta - a_{21}\left(\frac{\alpha}{a_{21}}\right)}{a_{22}-a_{21}\left(\frac{a_{12}}{a_{11}}\right)}\right)}{1 - a_{31}\left(\frac{a_{31}}{a_{11}}\right) - \left(a_{32}-a_{31}\left(\frac{a_{12}}{a_{11}}\right)\right)\times\left(\frac{1-a_{21}\left(\frac{1}{a_{11}}\right)}{a_{22}-a_{21}\left(\frac{a_{12}}{a_{11}}\right)}\right)}$.

Assuming that the function $I(x, y, 1) \in \mathbb{R}^3$ has at least three (3) derivatives, let $h_\star$ be a non-homogeneous step size, we opt to minimize the consistency error ε_i between the gradient and its estimate from the linear combination of the neighboring points as shown through Eq. 3.

$$\varepsilon_i = I_i^{(1)} - [\alpha I(x_i) + \beta I(x_i + h_d) + \gamma I(x_i - h_s)] \quad (3)$$

By substituting $I(x_i + h_d)$ and $I(x_i - h_s)$ with their Taylor series, this translates the consistency error into solving the following linear systems of equations as shown through Eq. 4 and the resulting approximation of $I_i^{(1)}$ is shown through Eq. 5.

$$\begin{cases} \alpha + \beta + \gamma = 0 \\ \beta h_d - \gamma h_s = 1 \\ \beta h_d^2 + \gamma h_s^2 = 0 \end{cases} \quad (4)$$

$$I_i^{(1)} = \frac{h_s^2 f(x_i + h_d) + (h_d^2 - h_s^2) I(x_i) - h_d^2 (x_i - h_s))}{h_s h_d (h_d + h_s)} + \mathcal{O}\left(\frac{h_d h_s^2 + h_s h_d^2}{h_d + h_s}\right) \quad (5)$$

When $h_\star$ is homogeneous step size indicating that $h_s = h_d$ the former Eq. 5 reduces to a simplified equation detailed through Eq. 6.

$$\frac{\hat{I}^{(1)}(x_{i+1}) - I(x_{i-1})}{2h} + \mathcal{O}(h^2) \quad (6)$$

From the above-optimized gradient, we use it to draw lines that are parallel to the long member or structure from the SRD. We finally, apply thresholds such as $0\%, 25\%, 50\%, 75\%$, and 100% of the white pixel values to obtain the central line with the center point (x, y) whose properties are similar to the long member of the SRD by learning through the white pixels as shown by Eq. 7.

$$(x, y) = \left(\max_{50 \le i < 75} \left(\frac{\hat{I}^{(1)}(x_{i+1}) - I(x_{i-1})}{2h}\right), \max_{50 \le i \le 75} \left(\frac{\hat{I}^{(1)}(y_{i+1}) - I(y_{i-1})}{2h}\right)\right) \quad (7)$$

Lastly, we present the proposed algorithm as shown in Fig. 2 with the description of each block and its essence. The workflow of the proposed algorithm has thirteen (13) steps whereby the block with "Input" defines a colored image which is converted to "Gray" in the second block for easy pixel manipulation. The third block with "Binarization" describes a binary image with small holes which are removed by applying iterative erosion and dilation to obtain a binary mask in the fourth block. The fifth block with "Contour Detection" determines the largest and external contour in a binary mask. In the sixth block, we obtain a "Convex Hull" by concatenating all contours to make one object such that a bounding rectangle can be obtained with four coordinates. The block with "Reference Point Assignment" transforms the initial point to the final point for the purpose of deducing the length and width of the SRD by allocating new coordinates in the ninth block. The block with "Multiple Lines" describes the sampled lines which are parallel to the long structure of the SRD from 0-100% sampled in four (4) steps to make parallel lines based on a backward war affine transformation. We then determine the center line by calculating the gradient in Eq. (6) and apply the minimum and maximum pixel value thresholds to constrain the white region with borders. Lastly, we determine the midpoint based on the lower and upper markers in a region between 25%, 50%, and 75% of the samples as shown through experiments.

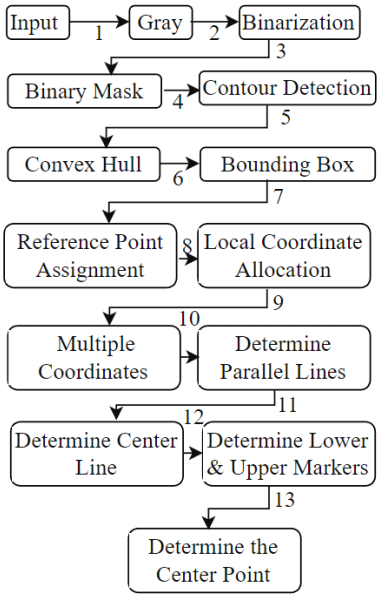

Fig. 2. Workflow for experiments of the proposed algorithm**.**

IV. Experimental Results

The experiments of this work were done through a gaming computer operating on windows 11 installed with python version 3.11. The analysis of the image features used "numpy" and OpenCV libraries whereby the former was used for pixel manipulations and the latter was used for output visualization. The following are the results from the proposed algorithm as shown in Fig. 3 and 4.

Fig. 3. Center point detection by the proposed algorithm.

To justify the authenticity of the proposed algorithm, we did an experiment for 25 images and compared it with the midpoint and centroid-based algorithm. We also assigned manually the midpoint by using ALsee software which gives the exact midpoint of an SRD. We limited the performance of the robot at 1mm error such that if it is out of bounds, then the robot would not grab and pick the SRD. For brevity purposes, we present the results for 6 images in tabular form as shown in Table 1 comparing the results for the proposed algorithm,

centroid, and center point-based algorithms to justify its authenticity.

Fig. 4. Center point detection by the proposed algorithm.

TABLE 1. COMPARATIVE RESULTS BASED ON ERRORS

Image	Algorithms		
	Centroid	***Midpoint***	***Proposed***
1	0.9614	0.9975	0.3741
2	1.8943	1.6528	0.5291
3	1.9651	1.4170	0.9537
4	0.9332	0.8669	0.8364
5	1.8817	1.2351	0.7934
6	2.3216	1.9954	0.2645
7	1.9513	2.0331	1.0873
8	0.9432	0.9512	0.1952
9	0.9924	0.9871	0.7515
10	0.9902	0.9873	0.8769

Based on the optimal threshold for center point determination, the proposed algorithm performed better than the two algorithms. Out of 25 images the proposed algorithm missed locating the center points of two images which is equivalent to an accuracy of 92% followed by the midpoint-based algorithm with an accuracy of 68% and the centroid-based algorithm achieved an accuracy of 45%. Based on the results from the proposed algorithm, we recommend the proposed algorithm be integrated with the open manipulator X algorithm for grabbing and picking SRD through the center and dispatching them to the assembling part.

V. CONCLUSION

In this study, we proposed an unsupervised machine-learning algorithm for a mobile robot to grab and pick an SRD through the center. The proposed algorithm uses image processing techniques for feature selection and extraction while integrating with backward inverse affine transformation to map the lines and parallelism regardless of the angle of rotation. Of many advantages the algorithm has, it is fast because it detects and locates the center point on an SRD for 0.025s and it has an accuracy of 92% compared to the center point and centroid-based algorithms. Additionally, the proposed algorithm works better than the centroid and midpoint-based algorithms as shown in Table 1.

.

Acknowledgment

This work was supported by the "Leaders in Industry-University Cooperation 3.0" of NRF, the basic research of NRF (NRF-2021R1F1A1062906), and the regional innovation cluster fostering project (R&DP004797) of the Korea Institute of Industrial Technology.

References

[1] B. Do and H. Lee, "Introduction of Shear Reinforcement of Dual-anchorage," Korean Structural Engineers Association, vol. 17, no. 5, pp. 63-66, 2010.

[2] P. Schmidt, M. Pleim, J. Bielak, and J. Hegger, "Activation Model for Various Punching Shear Reinforcement Types in Flat Slabs and Column Bases Optimized for Design," Engineering Structures, vol. 249, no. 113310, pp. 1-12, 2021.

[3] J. N. Mlyahilu, J. N. Mlyahilu, J.E. Lee, Y. B. Kim, and J. N. Kim, "Morphological Geodesic Active Contour Algorithm for the Segmentation of the Histogram-Equalized Welding Bead Image Edges," IET Image Processing, vol. 16, no. 10, pp. 2681-2696, 2022.

[4] J. N. Mlyahilu and J. N. Kim, "Welding Bead Segmentation Algorithm Using Edge Enhancement and Active Contour," The Korean Institute of Convergence and Signal Processing, vol. 21, no. 4, pp. 209-215, 2020.

[5] J. N. Mlyahilu, Y. B. Kim, J. E. Lee, and J. N. Kim, "An Algorithm of Welding Bead Detection and Evaluation Using Multiple Filters and Geodesic Active Contours," The Journal of Korean Institute of Convergence and Signal Processing, vol. 22, no. 3, pp. 141-148, 2021.

[6] P. Surlakar, S. Araujo, and K. M. Sundaram, "Comparative Analysis of K-Means and K-Nearest Neighbor Imaje Segmentation Techniques," IEEE International Conference on Advanced Computing, India, pp. 96-100, 2016.

[7] S. Srivastava, A. V. Divekar, C. Anilkumar, I. Naik, V. Kulkarni, and V. Pattabiraman, "Comparative Analysis of Deep Learning Image Detection Algorithms," Journal of Big Data, vol. 8, no. 66, pp. 1-27, 2021.

[8] R. Beutel, and J. Hegger, "The Effect of Anchorage on the Effectivess of the Shear Reinforcement in the Punching Zone," Cement and Concrete Composites, vol. 24, pp. 539-549, 2002.

[9] K. Kawamura, H. Nakamura, M. Takemura, and T. Miura, "Analytical Study on the Effect of Different Shear Reinforcement Shapes on Shear Failure Behaviour and Shear Resistance Mechanisim of RC Beams," Journal of Advanced Concrete Technology, vol. 19, pp. 571-584, 2021.

[10] J. N. Mlyahilu, Y. Kim, and J. N. Kim, "A Grab and Pick Algorithm for a Robot on Welding Beads," Conference of Korea Institute of Convergence and Signal Processing, pp. 54-55, Changwon, June, 2022.

[11] S. Oh and H. Ki, "Cross-Section Bead Image Prediction in Laser Keyhole Welding of AISI 1020 Steel Using Deep Learning Architectures," IEEE Access, vol. 8, pp. 73359-73372, 2020.

[12] D. Zhao, X. Hu, S. Xiong, J. Tian, J. Xiang, J Zhou, H. Li, "K-Means Clustering and KNN Classification Based on Negative Dataset," Applied Soft Computing, vol. 110, no. 107732, pp. 1-15, 2021.

[13] S. Ganjkoo, "YOLO and Mask R-CNN for Vehicle Number Plate Identification," Computer Vision and Pattern Recognition, Cornell University, pp. 1-8, 2022.

[14] K. Khan, A. Imran, H. Z. U. Rehman, A. Fazil, M. Zakwan, and Z. Mahmood, "Performance Enhancement Method for Multiple Licence Plate Recognition in Challenging Environment," EURASIP Journal on Image and Video Processing, vol. 30, pp. 1-23, 2021.